IIETA International Information and Engineering Technology Association
Advancing the World of Information and Engineering

Journal Européen des Systèmes Automatisés
Vol. 58, No. 2, February, 2025, pp. 317-327
Journal homepage: http://iieta.org/journals/jesa

Impact of STATCOM in Stabilizing Disturbed Microgrids Powered by Wind Energy

Habib Bali[1], Mohamed Boudiaf[2], Tayeb Allaoui[1], Karim Negadi[1*]

[1] Energy Engineering and Computer Engineering Laboratory (L2GEGI), University of Tiaret, Tiaret 14000, Algeria
[2] Renewable Energy Systems Applications Laboratory (LASER), University of Djelfa, Djelfa 17000, Algeria

Corresponding Author Email: karim.negadi@univ-tiaret.dz

https://doi.org/10.18280/jesa.580212

Received: 10 December 2024
Revised: 31 January 2025
Accepted: 19 February 2025
Available online: 28 February 2025

Keywords:
microgrid, wind energy, renewable energy integration, voltage stability, STATCOM

ABSTRACT

Electricity distribution systems face significant challenges, including energy losses, voltage instability, and the intermittency of renewable energy sources like wind and solar power. To enhance power quality and stability, advanced compensation devices such as Static Synchronous Compensator (STATCOM) are integrated into power networks. This paper investigates the impact of STATCOM on voltage regulation and wind energy integration within a 30 kV medium-voltage network at an interconnection point comprising a load, a renewable energy source, and an AC grid. A STATCOM-based control strategy is implemented to dynamically adjust voltage by injecting or absorbing reactive power, ensuring a stable power supply under various scenarios, including wind variations, load fluctuations, and short-circuit faults. Simulation results confirm that STATCOM effectively maintains voltage amplitude at its reference value, stabilizes the system during disturbances, and ensures continuous energy availability. By mitigating voltage variations and supporting renewable energy integration, STATCOM enhances overall power system reliability and quality.

1. INTRODUCTION

Distribution grids are essential components of modern electricity systems, acting as the bridge between transmission networks and end consumers. These grids ensure the reliable delivery of electricity generated in power plants to homes, businesses, and industrial facilities, thereby playing a critical role in supporting modern economies through a dependable and high-quality power supply [1].

However, electricity distribution networks face numerous challenges, including energy losses caused by conductor resistance and system inefficiencies [2], as well as the variability and intermittency of renewable energy sources such as solar and wind [3]. Additionally, maintaining the reliability and quality of electricity supply poses significant difficulties [4]. To address these issues and enhance the performance of distribution networks, various solutions have been proposed. These include the integration of renewable energy sources [5] and the improvement of voltage quality through compensation systems, such as advanced devices like STATCOM (Static Synchronous Compensator) [6].

STATCOM is a power electronics-based device that enhances the stability, quality, and reliability of electrical networks. As part of the Flexible AC Transmission Systems (FACTS) family, STATCOM optimizes the management of electrical power flows [7, 8]. It is particularly advantageous for networks incorporating renewable energy sources, such as wind and solar, which are characterized by intermittent power generation [9, 10].

This paper focuses on studying the impact of STATCOM on voltage quality and its effectiveness in facilitating the integration of wind turbines into a microgrid [11].

Several studies have explored this area. For instance, Lu and Rao [12] developed a STATCOM damper employing a recurrent Petri fuzzy probabilistic neural network to enhance transient stability in power systems with significant integration of offshore wind farms and photovoltaic plants. Similarly, studies [13, 14] extensively analyzed the challenges of voltage instability in wind-integrated power systems, covering its causes, effects, mitigation methods, and the role of grid codes in maintaining network security [15]. Moreover, Allaoui et al. [16] proposed using STATCOM to improve voltage quality and facilitate the integration of wind energy sources combined with storage systems.

Various conventional strategies, such as PI and PID controllers, have been proposed for controlling FACTS devices. Murali et al. conducted a comparative study of PI and PID controllers, focusing on performance parameters and closed-loop responses. Their simulation results demonstrated that the PID controller outperforms the PI controller in handling system disturbances. However, traditional control strategies have the limitation of being optimized for predefined operating conditions, which restricts their adaptability. To address these challenges, Pattnaik et al. [17] explored the integration of neuro-fuzzy controller (NFC) technology with STATCOM and SSSC. This approach aims to mitigate system disruptions and stabilize fixed-speed wind turbine systems based on synchronous generators in utility grids. Additionally, the study evaluated the impact of STATCOM on enhancing the stability of fixed-speed

synchronous generator-based wind energy systems under various operating conditions [18].

The remainder of this paper is structured as follows: Section 2 presents the system structure and modeling, detailing the microgrid configuration, wind turbine system, and STATCOM control strategy. Section 3 provides simulation results and analysis under different operating scenarios, including wind speed variations, load fluctuations, and short-circuit faults. Finally, Section 4 concludes the study by summarizing the key findings and highlighting the role of STATCOM in enhancing voltage stability and renewable energy integration within the microgrid.

2. STRUCTURE AND MODELING SYSTEM

2.1 Microgrid test

The microgrid analyzed in this study comprises a 230 kV fossil fuel power plant connected to the distribution network via a 230/30 kV step-down transformer. Additionally, the system includes a wind power plant equipped with a permanent magnet synchronous generator (PMSG) operating at 575 V, which is linked to the distribution network through a 575 V/30 kV step-up transformer. At the distribution network level, an electrical load is connected alongside a STATCOM, as illustrated in Figure 1.

In this study, microgrid configuration includes a 230 kV transmission network and a 575 V wind power plant. The 230 kV network aligns with real-world high-voltage systems, ensuring compatibility with large-scale power distribution and renewable energy integration. The 575 V wind power plant choice is based on practical implementation in Algeria, particularly in Adrar, and is commonly used in wind energy conversion due to IGBT-based power converter constraints. This configuration enhances the study's relevance by reflecting realistic operational conditions and facilitating the integration of renewable and conventional energy sources.

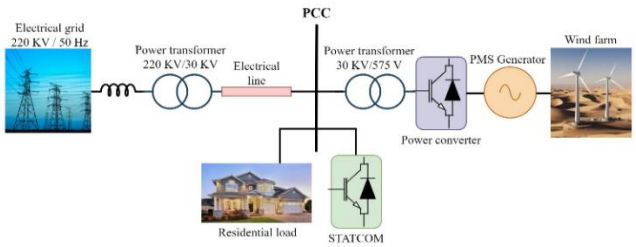

Figure 1. Configuration and basic design of the electrical network

This configuration ensures stable integration of renewable energy by regulating voltage fluctuations and balancing power flow. The STATCOM enhances grid reliability, ensuring continuous and efficient operation under varying conditions.

2.2 Modeling and control of wind turbine based MSAP

Figure 2 illustrates the complete system of a grid-connected Permanent Magnet Synchronous Generator wind turbine, which is equipped with a full back-to-back converter. In this configuration, the PMSG wind turbine operates without a gearbox, directly coupling the wind turbine to the generator. The generator's output is then connected to the electrical grid through a DC-link power converter, as shown in Figure 2, facilitating the transmission of power to the grid [19].

The subsequent differential equations are applicable for simulating the system dynamics of the PMSG wind turbine. The mechanical power extracted (P_{wt}) and the torque (T_{wt}) of the PMSG wind turbine are delineated as [20]:

$$\frac{di_d}{dt}=\frac{1}{L_d}v_d-\frac{R}{L_d}i_d+\frac{L_q}{L_d}p\omega_r i_q \tag{1}$$

$$\frac{di_q}{dt}=\frac{1}{L_q}v_q-\frac{R}{L_q}i_q+\frac{L_d}{L_q}p\omega_r i_d-\frac{\lambda p\omega_r}{L_d} \tag{2}$$

$$T_e=\frac{3}{2}p\left[\lambda i_q+\left(L_d-L_q\right)i_d i_q\right] \tag{3}$$

where, L denotes the inductance, R represents the resistance of the stator windings, i is the current, and v is the voltage. The subscripts d and q correspond to the direct and quadrature axes, respectively. The amplitude of the flux generated by the rotor's permanent magnets in the stator phases is denoted by λ, while p indicates the number of pole pairs [21]. The sinusoidal model assumes that the flux produced by the rotor's permanent magnets in the stator is sinusoidal, leading to sinusoidal electromotive forces.

The mechanical system's dynamics are governed by:

$$\frac{d\omega_r}{dt}=\frac{1}{J_g}(T_m-T_e-f\ \omega_r) \tag{4}$$

$$\omega_r=\frac{d\theta_r}{dt} \tag{5}$$

where, J_g represents the rotor's moment of inertia, f denotes the rotor's viscous friction, ω_r is the angular velocity, and T_m is the mechanical torque applied to the shaft.

Eqs. (1)-(5) for the PMSG in the wind turbine model describe the fundamental electrical and mechanical dynamics of the system. These equations capture the relationship between the generator's voltage, current, torque, and rotational speed, which are essential for understanding the conversion of wind energy into electrical power [22]. They also serve as the foundation for designing control strategies that optimize system performance and ensure stable operation under varying wind conditions.

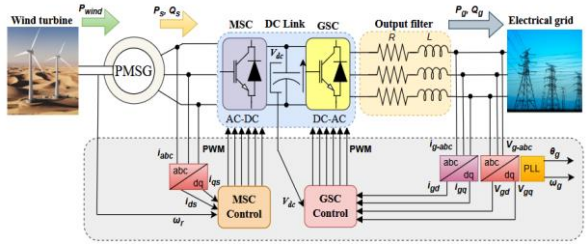

Figure 2. PMSG wind turbine with back-to-back power converter [23]

This system ensures efficient power conversion and integration of wind energy into the grid. The back-to-back converter regulates energy flow, optimizing performance and maintaining stability.

2.3 STATCOM modeling and control

As shown in Figure 3, the STATCOM used in this paper consists of a three-phase GTO-based Voltage Source Converter (VSC) and a DC capacitor (C). The STATCOM is connected to the transmission line through a step-down transformer, facilitating its integration into the system [24].

Figure 4 illustrates a single-phase equivalent circuit of the STATCOM, where V_{sh} represents the source voltage phasor. The transmission line is modeled with a resistance r_{sh} and inductance L_{sh}. The equivalent circuit simplifies the model by neglecting nonlinearities caused by the switching of semiconductor devices, transformer saturation, and controller time delays. It is also assumed that the transmission system is symmetrical for the purpose of this analysis [25].

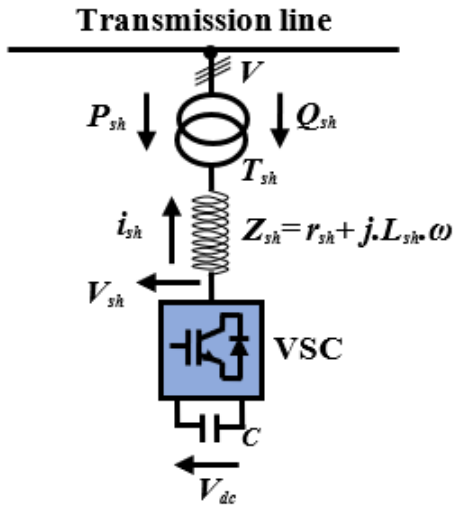

Figure 3. Basic layout of STATCOM

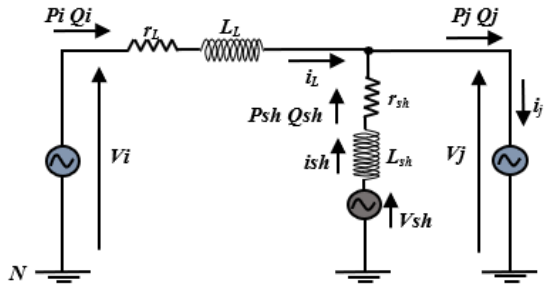

Figure 4. Equivalent circuit of STATCOM system

This analysis highlights the critical role of STATCOM in maintaining voltage stability and optimizing power flow. By dynamically adjusting reactive power, it ensures reliable grid operation, enhances power quality, and supports the integration of renewable energy sources [26].

The equations of the system in the model of Park transformation are:

$$\frac{d}{dt}\begin{bmatrix} i_{shd} \\ i_{shq} \end{bmatrix} = \begin{bmatrix} -\frac{r_{sh}}{L_{sh}} & \omega \\ -\omega & -\frac{r_{sh}}{L_{sh}} \end{bmatrix} \begin{bmatrix} i_{shd} \\ i_{shq} \end{bmatrix} + \frac{1}{L_{sh}} \left(\begin{bmatrix} V_{shd} \\ V_{shq} \end{bmatrix} - \begin{bmatrix} V_{sd} \\ V_{sq} \end{bmatrix} \right) \quad (6)$$

Eqs. (7) and (8) below give the active and reactive powers [27]:

$$P_{sh} = \frac{3}{2}\left(V_{shd} i_{shd} + V_{shq} i_{shq}\right) \quad (7)$$

$$Q_{sh} = \frac{3}{2}\left(V_{shd} i_{shq} - V_{shq} i_{shd}\right) \quad (8)$$

Figure 5 illustrates the overall schematic of the control circuits for the STATCOM system. This diagram provides a comprehensive view of the interconnected components responsible for regulating the device's operation. It highlights the key elements involved in voltage regulation, reactive power compensation, and system stability enhancement [28]. The control circuits are designed to ensure optimal performance under various operating conditions. This global representation serves as a foundation for understanding the STATCOM's functionality and its role in improving power quality.

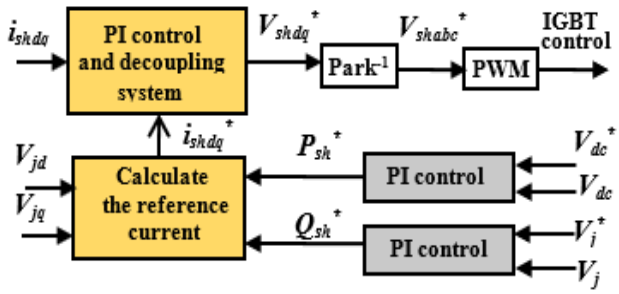

Figure 5. The block diagram of control circuit of STATCOM

The synthesis of d and q-axis currents i_d and i_q is essential for controlling active and reactive power and regulating voltage in power systems. The i_d current is synthesized to manage reactive power, directly influencing the voltage magnitude and ensuring stability under varying conditions. Similarly, the i_q current is synthesized to control active power flow, optimizing energy transfer between the source and the grid. The reference id and i_q current are given by [29]:

$$i_d^* = \frac{2}{3}\frac{(P_{sh}^* V_{shd} - Q_{sh}^* V_{shq})}{V_{shd}^2 + V_{shq}^2} \quad (9)$$

$$i_q^* = \frac{2}{3}\frac{(P_{sh}^* V_{shq} + Q_{sh}^* V_{shd})}{V_{shd}^2 + V_{shq}^2} \quad (10)$$

These currents are derived from reference values calculated based on the system's power and voltage requirements [30]. Advanced control algorithms, such as PI or sliding mode controllers, ensure that the synthesized currents track their references precisely, enabling efficient and stable operation of the system.

3. SIMULATION RESULTS AND ANALYSIS

Figure 6 shows the energy path at the load node (P_L = 8.2 MW and Q_L=2 MVAR).

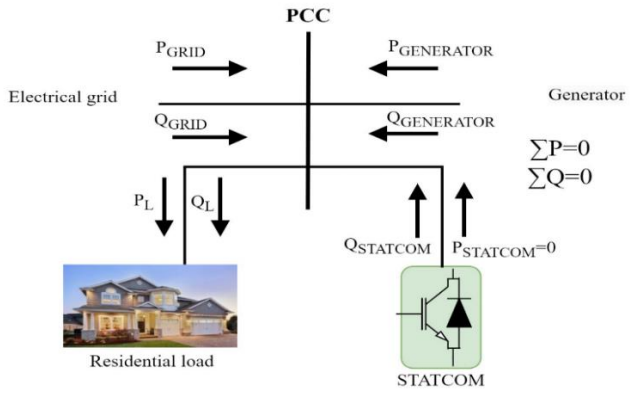

Figure 6. The energy path at the load node

The high performance of this modest modernization will be justified by the application of the following three tests scenario:

- Wind speed variation;
- Load variation;
- Appearance of a short-circuit fault.

The parameters used for the simulation are presented in Table 1 and Table 2. These tables provide detailed values for the various system components and control parameters, which are crucial for the analysis and performance evaluation of the modeled system.

Table 1. STATCOM parameters

Parameters	Values
STATCOM Resistance	R_{sh} =1 Ω
STATCOM Resistance	C_{sh}=0.002 F
STATCOM Inductance	L_{sh} =0.001 H
DC Voltage	2400 Volts
DC Voltage Regulation	K_p=0.001, K_i=0.15
Current Regulation	K_p=0.8, K_i=200
AC Voltage Regulation	K_p=0.55, K_i=250

Table 2. Wind turbine parameters

Parameters	Values
Rated power	3*3 MW
Rated voltage	575 V
DC capacity	$10000*10^{-6}$ F
Based DC voltage	1150 V
X	0.003 pu
R	0.3 pu
L_d	$0.3*10^{-3}$ H
L_q	$0.3*10^{-3}$ H
J_g	35000 kg.m^2
f	0.01 N.m.s
p	48

3.1 Scenario of wind speed variation

The aerodynamic disturbance is implemented by the variation of wind speed from 12 m/sec to 8m/sec for 5 sec. Figure 7 represents the decrease in voltage drop in the absence of the STATCOM compensator, but on the other hand in the presence of the STATCOM the voltage amplitude always returns to the reference value whatever the variation of the wind, because the STATCOM is a very powerful voltage regulator, especially in static mode.

As shown in Figure 8 the decrease of the generated power due to the decrease of the wind (using MPPT control), and the generated reactive power remains zero under the order of the control, consequently to decrease the amplitude of the generated current. The wind generator must be controlled by the MPPT (P&O) strategy to generate the Max power to the load and the interconnection power network.

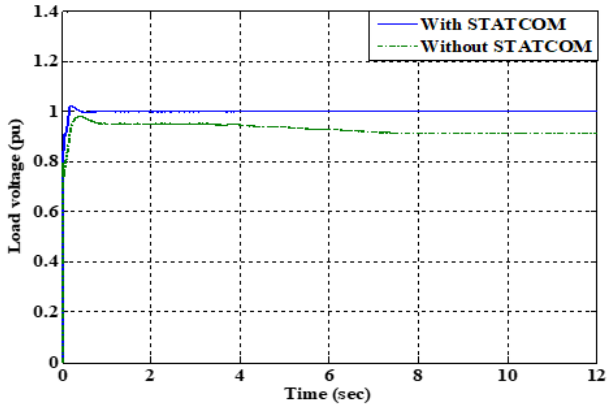

Figure 7. Load voltage variation

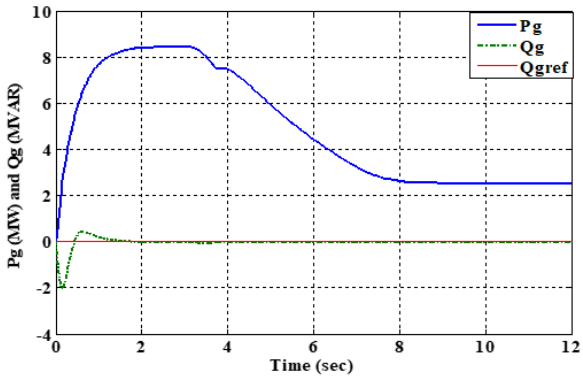

Figure 8. Active and reactive power generated by wind generator

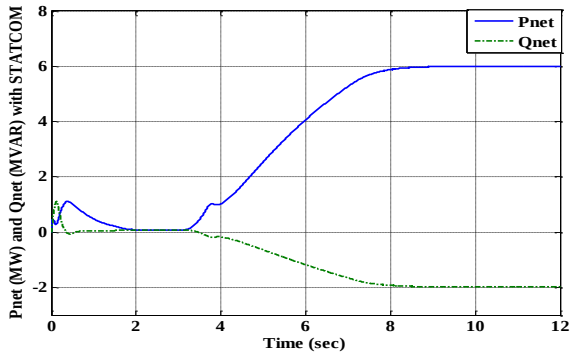

Figure 9. Active and reactive power generated by power network (with STATCOM)

Figure 9 illustrates the dynamic behavior of energy delivery from the electrical network to the load in the presence of a STATCOM. Through their reactive injection and voltage adjustment capacity, the STATCOM actively regulates the power flow, ensuring that the network injects sufficient electrical energy to compensate for any shortfall at the load level. This compensation helps maintain a stable and continuous energy supply, even under varying load demands or network conditions. Correct power supply with electrical energy requires correct voltage regulation (without voltage drop or overvoltage).

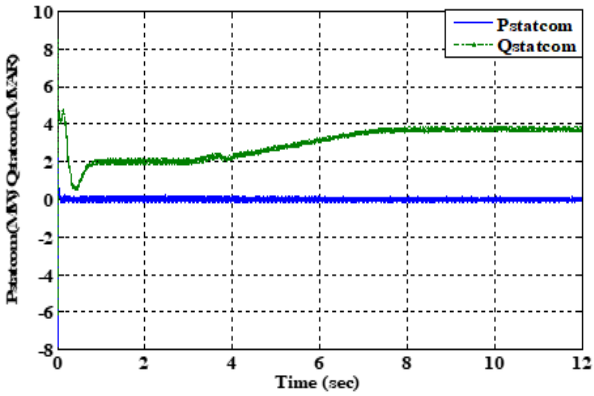

Figure 10. Injected active and reactive power by STATCOM

As shown in Figure 10, the STATCOM injects reactive power into the load to regulate the voltage at the load node while ensuring that no active power is injected.

Figure 11 highlights the advantage of STATCOM in maintaining a stable power supply to the load, even during fluctuations in wind speed, whether there is a decrease or increase in wind energy generation. This enables the system to adapt to changing conditions and continue supplying the necessary energy to the load. In the presence of STATCOM, the active and reactive powers requested by the load will always be ensured regardless of the wind variation. In the absence of STATCOM on the test system, the power generated by the electrical network, both active and reactive, varies randomly, as shown in Figure 12.

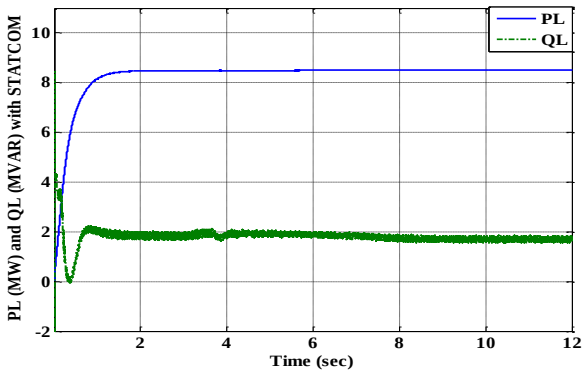

Figure 11. Active and reactive power Load (with STATCOM)

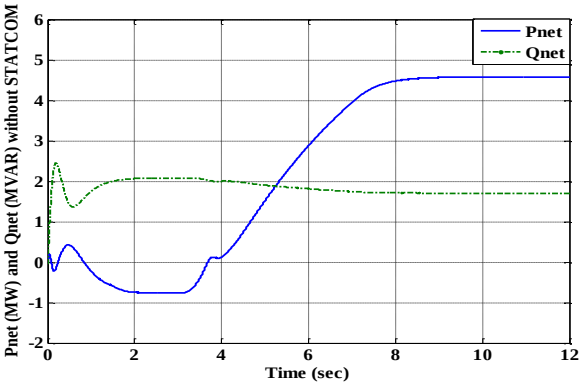

Figure 12. Active and reactive power generated by power network (without STATCOM)

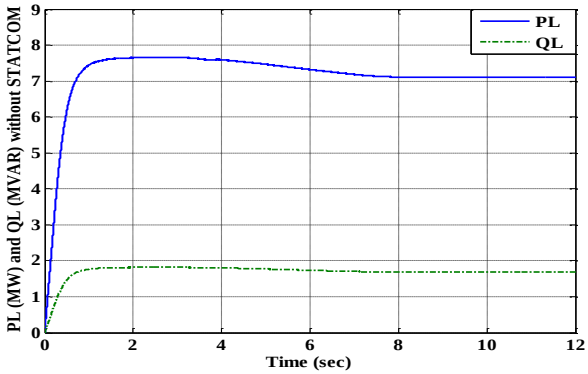

Figure 13. Active and reactive power load (without STATCOM)

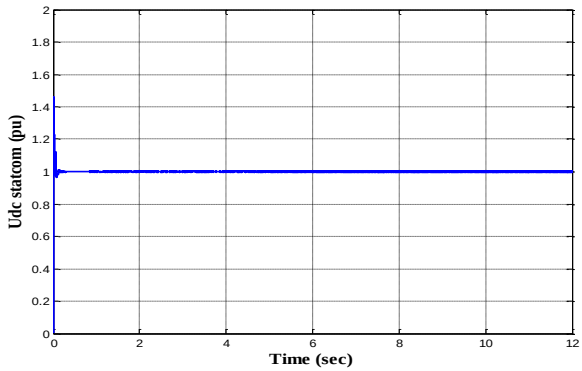

Figure 14. DC Voltage of STATCOM

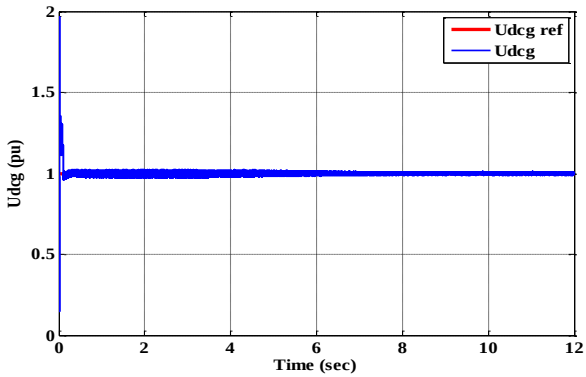

Figure 15. DC Voltage of wind generator

This instability leads to an energy deficit at the load, as depicted in Figure 13, caused by a voltage collapse, which is further illustrated in Figure 7. Without STATCOM's compensation, the network struggles to maintain a consistent power supply, resulting in inadequate energy delivery to the load. Figures 14 and 15 successively represent the maintenance of the DC voltage on the STATCOM DC bus and the wind generator DC bus.

3.2 Scenario of load variation

Now the load is adjusted up to 12 MW and 4 MVAR from 3 sec to 5 sec, there are 03-time intervals:

- Interval 1: P_L = 8.2 MW and Q_L = 2 MVAR for t<3 sec.

- Interval 2: P_L = 12 MW and Q_L = 4 MVAR for 3 sec < t < 5 sec.
- Interval 3: P_L = 8.2 MW and Q_L=2 MVAR for t>5 sec (return to initial state).

As shown in Figure 16, the presence of STATCOM ensures that the grid voltage is maintained during the three load variation time intervals. As shown in Figure 16, the presence of STATCOM ensures the maintenance of the charging voltage during the three time intervals, even with minimal disturbances at the moments of disturbance. In contrast, in the absence of STATCOM, there are significant voltage drops during these three intervals, particularly in the second interval when the load increases, resulting in unacceptable voltage levels.

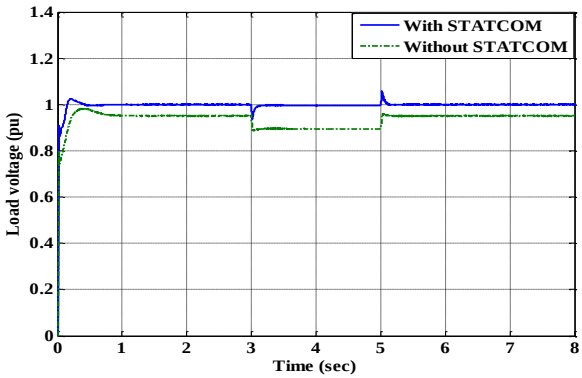

Figure 16. Load voltage variation

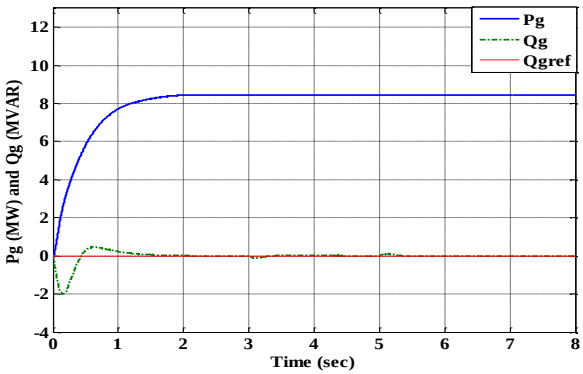

Figure 17. Active and reactive power generated by wind generator

Figure 17 demonstrates that the active and reactive power of the load remains constant, controlled by the MPPT algorithm, regardless of load variations. This stability is maintained both with and without the presence of the STATCOM. This is justified by the total independence between the control of the wind generator using MPPT regulation and the electrical micro-grid, whatever the disturbances on the AC power grid side. As previously mentioned in Figure 16, the STATCOM maintains the load bus voltage at its reference value, ensuring dynamic adjustment to meet the power demands of the electrical network. As shown in Figure 18, this regulation involves either increasing or decreasing the injected power as needed. Figure 19 illustrates the variation in reactive power injected by the static compensator in response to changes in the load. The presence of the STATCOM compensator ensures load stability across the three time intervals, as shown in Figure 20.

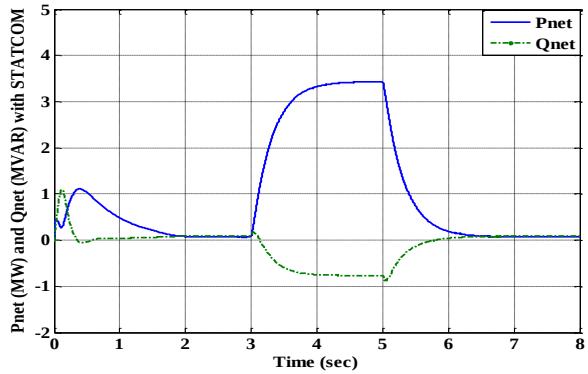

Figure 18. Active and reactive power generated by power network (with STATCOM)

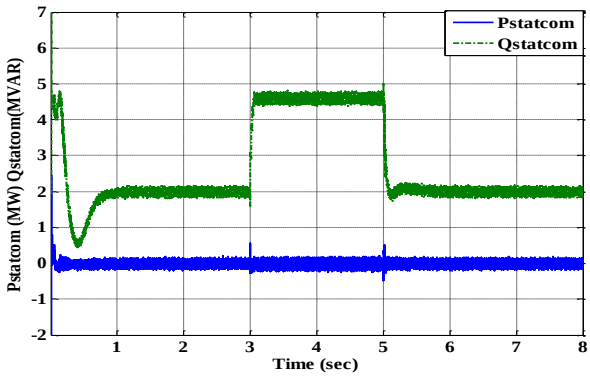

Figure 19. Injected active and reactive power by STATCOM

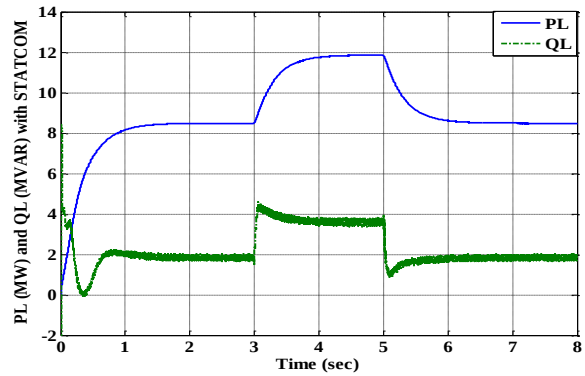

Figure 20. Active and reactive power load (with STATCOM)

The power generated by the network-wind generator system precisely matches the power required by the load. In this configuration, the compensator acts as an electric pump, maintaining balance. The STATCOM absorbs minor active power transients primarily to charge the capacitor. As depicted in Figure 19, the reactive power supplied by the STATCOM matches the reactive power demanded by the load, as illustrated in Figure 20, ensuring a power factor of 1 at the load.

Figure 21 highlights the instability and erratic energy fluctuations that occur in the absence of the compensator. This results in random power variations due to a voltage drop at the load bus. Additionally, as shown in Figure 22, the electrical network injects active and reactive power inconsistently toward the load.

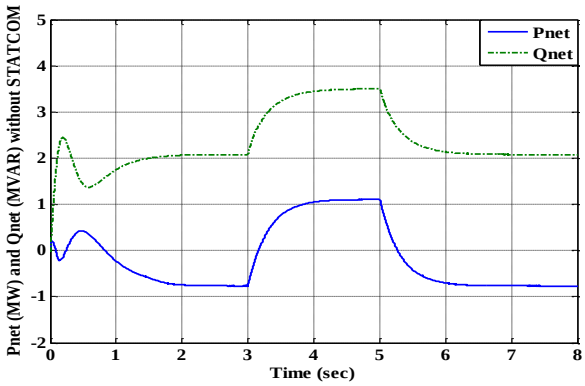

Figure 21. Active and reactive power generated by power network (without STATCOM)

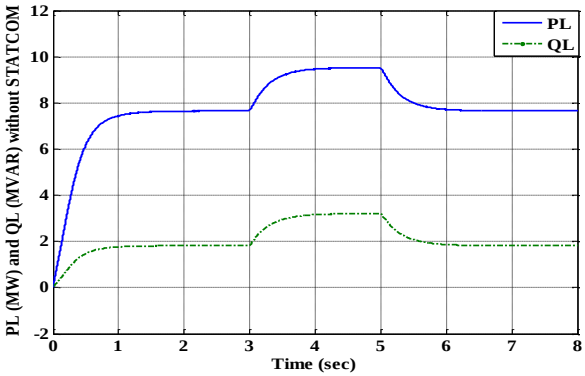

Figure 22. Active and reactive power Load (without STATCOM)

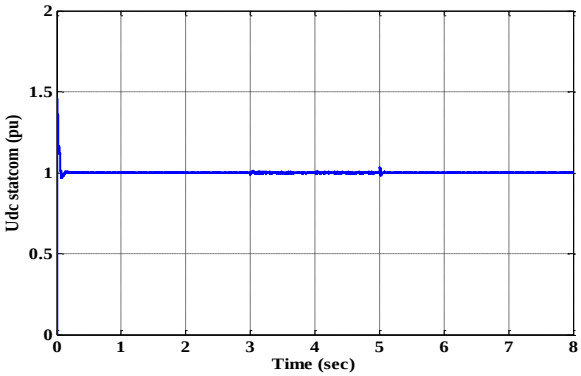

Figure 23. DC Voltage of STATCOM

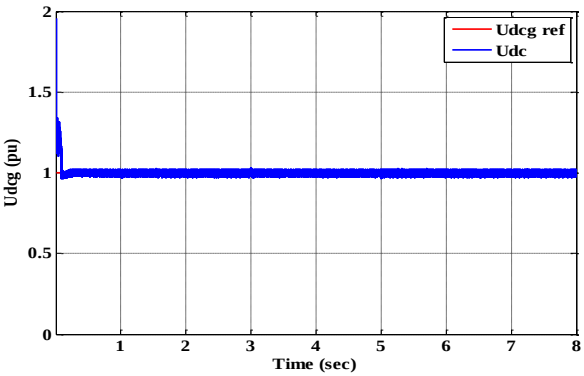

Figure 24. DC Voltage of wind generator

To maintain system stability, conventional control circuits regulate the DC voltage, aligning it with the STATCOM compensator's setpoint and stabilizing the wind generator, as illustrated in Figures 23 and 24.

3.3 Scenario of short-circuit fault application

In the event of a three-phase short-circuit fault on the power line at 3 seconds, the fault will be cleared by opening the line at 3.2 seconds (with a fault duration of 200 milliseconds), isolating the power grid. At this point, the only source available to supply the load is the wind generator. As shown in Figure 25, in the presence of static compensation, the voltage quickly returns to its initial equilibrium state despite the transient disturbance. In contrast, without compensation, a significant voltage drop occurs during the transient period.

The wind generator supplies active power to the load, while the STATCOM provides reactive power, as shown in Figure 26 (a). In the absence of STATCOM, the energy system forces the wind conversion chain to generate reactive power for the load, leading to degradation in control and loss of reactive power regulation, as illustrated in Figure 26 (b). With the STATCOM in place, the active power generated by the electrical network remains zero before and after the fault clearance, as shown in Figure 27. This is due to the energy availability from the wind turbine and the stable voltage at the load.

The STATCOM continues to generate reactive power for the load, as shown in Figure 28, and ensures stability and energy availability throughout the fault clearance process.

Figure 29 explains the main objective of this work, the use of the static reactive power compensator STATCOM to help the wind generator to supply the load with the necessary energy needs.

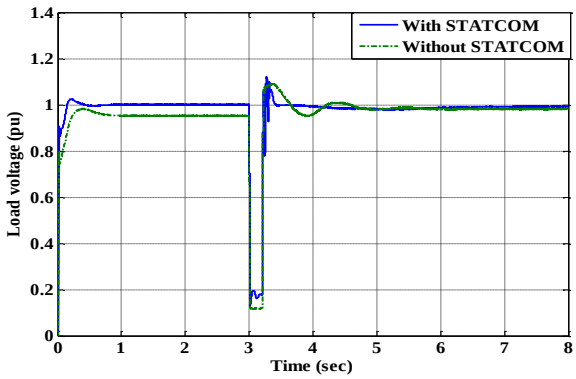

Figure 25. Load voltage variation

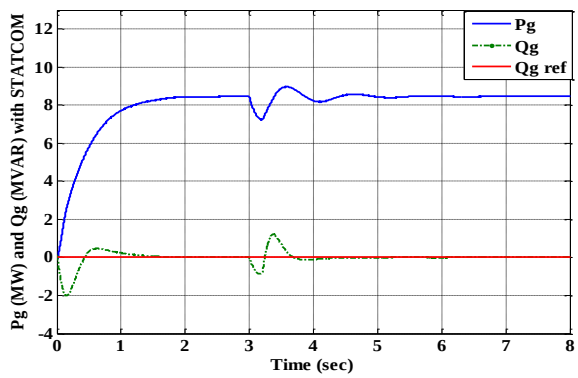

(a) With STATCOM

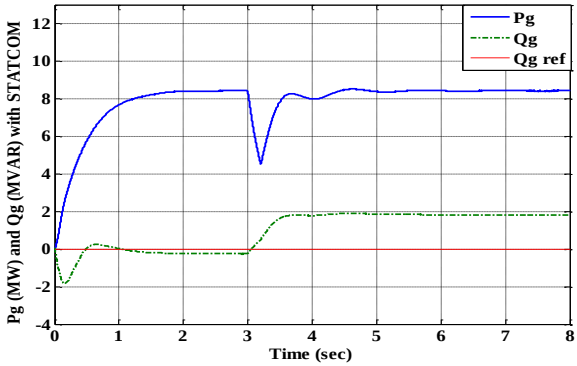

(b) Without STATCOM

Figure 26. Active and reactive power generated by wind generator

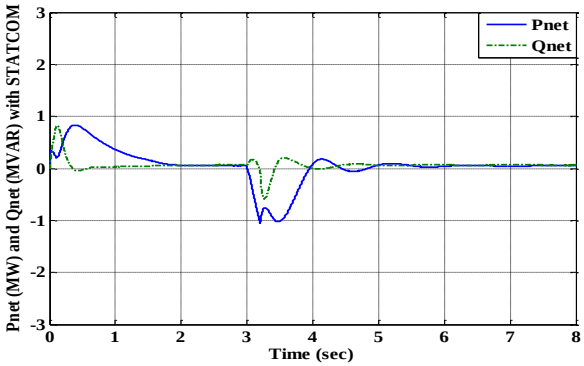

Figure 27. Active and reactive power generated by power network (with STATCOM)

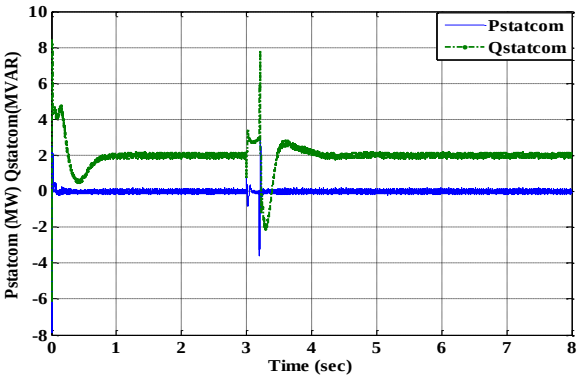

Figure 28. Injected active and reactive power by STATCOM

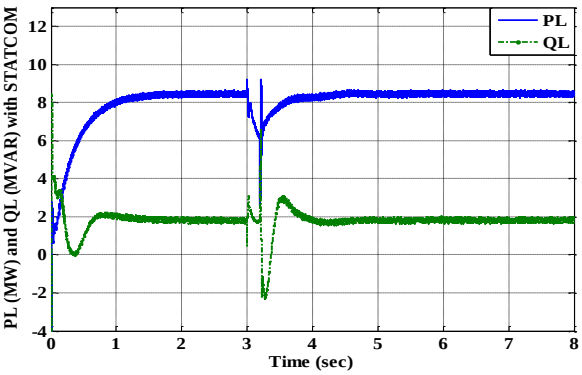

Figure 29. Active and reactive power load (with STATCOM)

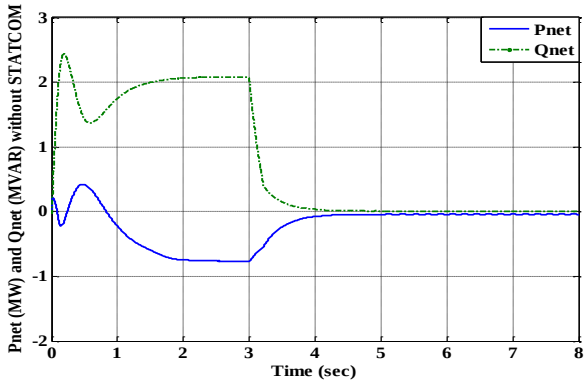

Figure 30. Active and reactive power generated by power network (without STATCOM)

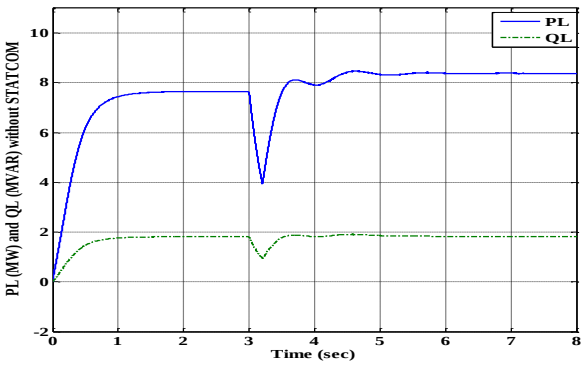

Figure 31. Active and reactive power load (without STATCOM)

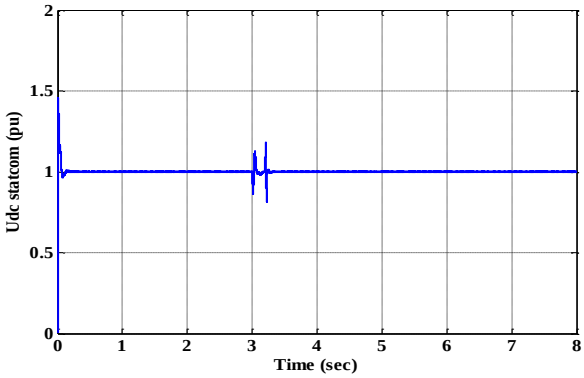

Figure 32. DC Voltage of STATCOM

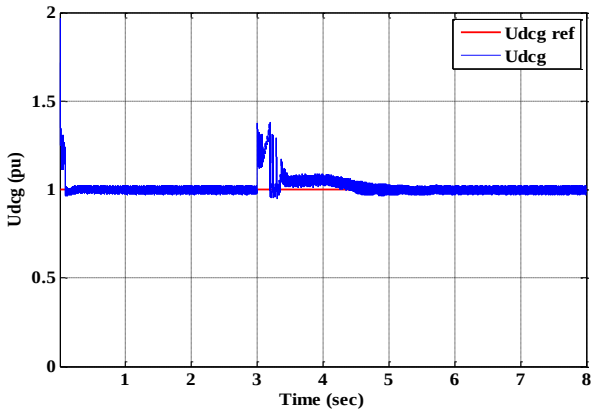

Figure 33. DC Voltage of wind generator

This figure shows the values of the powers generated by the grid-wind generator group equal to the demand of the load before and after the elimination of the power grid due to fault: This is the decentralization of the electrical network with the autonomy of energy production.

As shown in Figure 30, the active and reactive powers generated by the power network are cancelled during and after the elimination of the short-circuit fault by opening the line through the circuit breaker, which implies an energy shortage in the load, this caused by the degradation of the voltage quality on the load bus. Figure 31 describes the energy behavior of the load without STATCOM, highlighting the imbalance between production and consumption resulting from the voltage collapse.

Figures 32 and 33 depict the restoration of voltage regulation on the STATCOM's DC buses and the wind conversion chain after the fault has been cleared, showing the system's recovery and stabilization following the disturbance.

4. CONCLUSIONS

This study examined the integration of a STATCOM into a wind-powered microgrid to enhance voltage stability and overall system reliability. Through three simulation scenarios—wind speed variations, load fluctuations, and short-circuit faults—the impact of STATCOM on power quality and grid resilience was thoroughly analyzed. The results demonstrated that STATCOM effectively regulates voltage amplitude, ensuring rapid restoration to its reference value despite wind speed variations. It dynamically adjusts reactive power injection to counteract load fluctuations, preventing voltage instability and maintaining power balance. During fault conditions, STATCOM significantly enhances grid resilience by providing reactive power support, accelerating voltage recovery, and ensuring continuous power supply. These findings underscore the critical role of STATCOM in improving the integration of renewable energy sources into microgrids, mitigating the challenges associated with their intermittency. Future research could focus on advanced control strategies, such as adaptive and predictive algorithms, to further optimize STATCOM performance in dynamic grid environments. Additionally, experimental validation and large-scale implementation would provide deeper insights into its real-world applicability for enhancing power system stability and reliability.

REFERENCES

[1] Deka, D., Kekatos, V., Cavraro, G. (2024). Learning distribution grid topologies: A tutorial. IEEE Transactions on Smart Grid, 15(1): 999-1013. https://doi.org/10.1109/TSG.2023.3271902

[2] Koulali, M., Negadi, K., Berkani, A., Aimer, A.F., Marignetti, F., Ertan, H.B. (2023). Advanced control of eleven level modular converter connected to the power grid via HVDC transmission line. In 2023 International Aegean Conference on Electrical Machines and Power Electronics (ACEMP) & 2023 International Conference on Optimization of Electrical and Electronic Equipment (OPTIM), Istanbul, Turquie, pp. 1-10. https://doi.org/10.1109/ACEMPOPTIM57845.2023.10287027

[3] Osmani, K., Haddad, A., Lemenand, T., Castanier, B., Alkhedher, M., Ramadan, M. (2023). A critical review of PV systems' faults with the relevant detection methods. Energy Nexus, 100257. https://doi.org/10.1016/j.nexus.2023.100257

[4] Ahmed, M.M.R., Mirsaeidi, S., Koondhar, M.A., Karami, N., et al. (2024). Mitigating uncertainty problems of renewable energy resources through efficient integration of hybrid solar PV/wind systems into power networks. IEEE Access, 12: 30311-30328. https://doi.org/10.1109/ACCESS.2024.3370163

[5] Boudali, A., Negadi, K., Bouradi, S., Berkani, A., Marignetti, F. (2021). Design of nonlinear backstepping control strategy of PMSG for hydropower plant power generation. Journal Européen des Systèmes Automatisés, 54(1): 1-8. https://doi.org/10.18280/jesa.540101

[6] Mekki, M., Boulouiha, H.M., Allali, A., Denai, M. (2021). Impact of the integration of a STATCOM controlled by LQG/H2 regulator in an energy system. European Journal of Electrical Engineering, 23(5): 361-370. https://doi.org/10.18280/ejee.230502

[7] Hamdan, I., Ibrahim, A.M.A., Noureldeen, O. (2020). Modified STATCOM control strategy for fault ride-through capability enhancement of grid-connected PV/wind hybrid power system during voltage sag. SN Applied Sciences: 2: 364. https://doi.org/10.1007/s42452-020-2169-6

[8] Sarwar, M., Arshed, M., Hussain, B., Rasheed, M., Tariq, H., Czapp, S., Tariq, S., Sajjad, I.A. (2023). Stability enhancement of grid-connected wind power generation system using PSS, SFCL and STATCOM. IEEE Access, 11: 30832-30844. https://doi.org/10.1109/ACCESS.2023.3262172

[9] Borousan, F., Hamidan, M.A. (2023). Distributed power generation planning for distribution network using chimp optimization algorithm in order to reliability improvement. Electric Power Systems Research, 217: 109109. https://doi.org/10.1016/j.epsr.2022.109109

[10] Malik, F.H., Khan, M.W., Rahman, T.U., Ehtisham, M., Faheem, M., Haider, Z.M., Lehtonen, M. (2024). A comprehensive review on voltage stability in wind-integrated power systems. Energies, 17(3): 644. https://doi.org/10.3390/en17030644

[11] Kataray, T., Nitesh, B., Yarram, B., Sinha, S., Cuce, E., Shaik, S., Roy, A. (2023). Integration of smart grid with renewable energy sources: Opportunities and challenges-A comprehensive review. Sustainable Energy Technologies and Assessments, 58: 103363. https://doi.org/10.1016/j.seta.2023.103363

[12] Lu, K.H., Rao, Q. (2023). Enhancing the dynamic stability of integrated offshore wind farms and photovoltaic farms using STATCOM with intelligent damping controllers. Sustainability, 15(18): 13962. https://doi.org/10.3390/su151813962

[13] Mumtahina, U., Alahakoon, S., Wolfs, P. (2023). A literature review on the optimal placement of static synchronous compensator (STATCOM) in distribution networks. Energies, 16(17): 6122. https://doi.org/10.3390/en16176122

[14] Shukla, V., Mukherjee, V., Singh, B. (2023). Integration of distributed generations and static var compensators with static synchronous compensators to reduce power losses. Engineering Applications of Artificial Intelligence, 126: 107208.

https://doi.org/10.1016/j.engappai.2023.107208
[15] Koulali, M., Berkani, A., Negadi, K., Mankour, M., Mezouar, A. (2020). Sliding fuzzy controller for energy management of residential load by multi-sources power system using wind PV and battery. Journal Européen des Systèmes Automatisés, 53(3): 305-315. https://doi.org/10.18280/jesa.530301
[16] Allaoui, T., Denaï, M.A., Bouhamida, M. (2007). Robust control of unified power flow controller (UPFC). Journal of Electronic and Electrical Engineering (IU-JEEE).
[17] Pattnaik, A., Dauda, A.K., Panda, A. (2023). Optimal utilization of clean energy and its impact on hybrid power systems incorporating STATCOM and pumped hydro storage. Renewable and Sustainable Energy Reviews, 187: 113713. https://doi.org/10.1016/j.rser.2023.113713
[18] Koulali, M., Negadi, K., Mankour, M., Mezouar, A., Berkani, A., Boumediene, B. (2019). Adaptive fuzzy control of hybrid PV/fuel cell and battery system using three-level t type inverter. Przegląd Elektrotechniczny, 95(12): 25-31.
[19] Sabo, A., Abdul Wahab, N.I., Othman, M.L., Mohd Jaffar, M.Z.A., Beiranvand, H., Acikgoz, H. (2021). Application of a neuro-fuzzy controller for single machine infinite bus power system to damp low-frequency oscillations. Transactions of the Institute of Measurement and Control, 43(16): 3633-3646. https://doi.org/10.1177/01423312211042781
[20] Araria, R., Guemmour, M.B., Negadi, K., Berkani, A., Marignetti, F., Bey, M. (2024). Design and evaluation of a hybrid offshore wave energy converter and floating photovoltaic system for the region of Oran, Algeria. Electrical Engineering & Electromechanics, (6): 11-18. https://doi.org/10.20998/2074-272X.2024.6.02
[21] Zhao, F., Wang, X., Zhou, Z., Meng, L., et al. (2023). Energy-storage enhanced STATCOMs for wind power plants. IEEE Power Electronics Magazine, 10(2): 34-39. https://doi.org/10.1109/MPEL.2023.3273893
[22] Okedu, E.K. (2023). Investigating permanent magnet synchronous generator wind turbine performance during low voltage using series and bridge type fault current limiters. ELECTRICA, 23: 212-221. https://doi.org/10.5152/electrica.2022.22066
[23] Adware, R., Chandrakar, V. (2023). Power quality enhancement in a wind farm connected grid with a fuzzy-based STATCOM. Engineering, Technology & Applied Science Research, 13(1): 10021-10026. https://doi.org/10.48084/etasr.5474
[24] Berkani, A., Pourkeivannour, S., Negadi, K., Boumediene, B., Allaoui, T., Ertan, H.B. (2019). Integration of offshore wind farm plants to the power grid using an HVDC line transmission. In 2019 International Aegean Conference on Electrical Machines and Power Electronics (ACEMP) & 2019 International Conference on Optimization of Electrical and Electronic Equipment (OPTIM), Istanbul, Turkey, pp. 486-492. https://doi.org/10.1109/ACEMP-OPTIM44294.2019.9007223
[25] Sami, I., Ullah, S., Ullah, N., Ro, J.S. (2021). Sensorless fractional order composite sliding mode control design for wind generation system. ISA Transactions, 111: 275-289
[26] Harrouz, A., Korhan, K., Becheri, H., Ilhami, C. (2022). Power Stabilization with STATCOM on DFIG Based Wind Farm for Renewable Energy. Algerian Journal of Renewable Energy and Sustainable Development, 4(1), 84-93. https://asjp.cerist.dz/en/article/232724
[27] Kuang, H., Zheng, L., Li, S., Ding, X. (2019), Voltage stability improvement of wind power grid-connected system using TCSC-STATCOM control. IET Renewable Power Generation, 13: 215-219. https://doi.org/10.1049/iet-rpg.2018.5492
[28] Rahmani, M., Faghihi, F., Moradi CheshmehBeigi, H., Hosseini, S.M. (2018). Frequency Control of Islanded Microgrids Based on Fuzzy Cooperative and Influence of STATCOM on Frequency of Microgrids. Journal of Renewable Energy and Environment, 5(4): 27-33. https://doi.org/10.30501/jree.2018.94119
[29] Mahmoud, M.M., Salama, H.S., Bajaj, M., Aly, M.M., Vokony, I., Bukhari, S.S.H., Wapet, D.E.M., Abdel-Rahim, A.M. (2023). Integration of wind systems with SVC and STATCOM during various events to achieve FRT capability and voltage stability: Towards the reliability of modern power systems. International Journal of Energy Research, 2023(1): 8738460. https://doi.org/10.1155/2023/8738460
[30] Yahia, S., Taha, R., Ayachi, E. (2024). Wind conversion systems effects on power grid and ability of thyristor controlled series capacitor and static synchronous series compensator devices for dynamic performance enhancing. Measurement and Control, 00202940241268714. https://doi.org/10.1177/00202940241268714

NOMENCLATURE

d	The direct axis
f	The rotor's viscous friction (N.m.s)
i	The current (A)
J_g	The rotor's moment of inertia (kg·m²)
L	The inductance (H)
L_{sh}	The inductance of the transmission line (H)
p	The number of pole pairs
P_L	The active power load (W)
P_{wt}	The mechanical power extracted from PMSG (W)
q	The quadrature axis
Q_L	The reactive power load (VAR)
R	The resistance of the stator windings (Ω)
r_{sh}	The resistance of the transmission line (Ω)
T_m	The mechanical torque applied to the shaft (N.m)
T_{wt}	The torque of the PMSG (N.m)
v	The voltage (V)

Greek symbols

λ	The amplitude of the flux generated by the rotor's permanent magnets in the stator phases (Wb)
ω_r	The angular velocity (rad/s)

Subscripts

AC	Alternative current
DC	Direct current
FACTS	Flexible AC transmission systems
NFC	Neuro-fuzzy controller

PCC	Point of common coupling	STATCOM	Static synchronous compensator
PMSG	Permanent magnet synchronous generator	VSC	Voltage source converter